Supporting Information for

Tumor-Specific Formation of Enzyme Instructed Supramolecular Self-Assemblies as Cancer Theranostics

Peng Huang[1,5], Yuan Gao*[2,3], Jing Lin[1,4], Hao Hu[1], Hsien-Shun Liao[4], Xuefeng Yan[1], Yuxia Tang[1], Albert Jin[4], Jibin Song[1], Gang Niu[1], Guofeng Zhang[4], Ferenc Horkay[2], Xiaoyuan Chen*[1]*

[1]Laboratory of Molecular Imaging and Nanomedicine (LOMIN), National Institute of Biomedical Imaging and Bioengineering (NIBIB), National Institutes of Health, Bethesda, Maryland 20892, United States

[2]Section on Tissue Biophysics and Biomimetics, Program on Pediatric Imaging and Tissue Sciences, Eunice Kennedy Shriver National Institute of Child Health and Human Development, National Institutes of Health, Bethesda, Maryland 20892, United States

[3]Beijing Engineering Research Center for BioNanotechnology and CAS Key Lab for Biological Effects of Nanomaterials and Nanosafety, National Center for NanoScience and Technology, No., 11 Zhongguancun Beiyitiao, Beijing 100190, China

[4]Laboratory of Cellular Imaging and Macromolecular Biophysics, National Institute of Biomedical Imaging and Bioengineering (NIBIB), National Institutes of Health, Bethesda, Maryland 20892, United States

[5]Department of Biomedical Engineering, School of Medicine, Shenzhen University, Guangdong Key Laboratory for Biomedical Measurements and Ultrasound Imaging, Shenzhen 518060, China

Corresponding authors: P. Huang (peng.huang@nih.gov); Y. Gao (gaoy@nanoctr.cn); X. Chen (shawn.chen@nih.gov)

EXPERIMENTAL SECTION

Characterization. The morphologies of all the samples were determined by transmission electron microscopy (TEM) and atomic force microscopy (AFM). TEM sample preparation: (1) 3 L of sample solution/gel was placed on the copper grid. (2) 30 sec later, a large drop of the water was placed on Parafilm® film and the sample on the grid was allowed to contact the water drop; the grid was tilted by 90 degrees and the water was gently absorbed from the edge of the grid using a filter paper. (3) A large drop of the UA stain solution was placed on parafilm and the grid was touched to the stain solution drop, with the sample-loaded surface facing the parafilm; the grid was tilted and the stain solution was gently absorbed from the edge of the grid using a filter paper sliver (3 times). (4) The grid was allowed to dry in air and the grid was examined as soon as possible. TEM were conducted on the FEI Tecnai12 transmission electron microscope (FEI, Hillsboro, Oregon) operating at an accelerating voltage of 120 kV. Images were acquired using a Gatan 2k X 2k cooled CCD camera (Gatan, Pleasanton, CA).

Samples for AFM were prepared by casting 3-10 μL of sample aqueous solution on freshly peeled mica substrate and rinsing, drying and dehumidifying. AFM imaging was conducted in air, using gentle tapping-mode AFM with a PicoForce Multimode AFM (Bruker, CA) consisting of a Nanoscope® V controller, a type E scanner head, and a sharpened TESP-SS (Bruker, CA) or similar AFM cantilever. AFM images were then analyzed by Nanoscope softwares (ver. 7.3-8.15, Bruker, CA).

Hydrodynamic diameters of samples were measured by a SZ-100 nano particle analyzer (HORIBA Scientific, Tokyo, Japan). Fluorescence emission spectra were recorded on an F-7000 fluorescence spectrophotometer (Hitachi, Tokyo, Japan). CD spectra were recorded on a Jasco J-815 spectropolarimeter.

Cell culture. Human cervical carcinoma HeLa cell line and 4T1 murine breast cancer cell line were bought from American Type Culture Collection (ATCC), cultured in standard cell media, and incubated at 37 °C in a humidified 5% CO_2 incubator.

Cellular formation of nanofiber. To investigate the cellular formation of nanofiber, HeLa cells were seeded at a density of 5000 cells per well in 96-well plates for 24 h, and then incubated with different samples: **1** at 10 μg/mL; **2** at 500 μg/mL; **1** at 10 μg/mL + **2** at 500 μg/mL; **1** at 10 μg/mL + **2** at 500 μg/mL + 5 μmol/L CinnGEL 2Me in 0.1% DMSO, respectively. The optical density (OD) changes of cells at 780 or 808 nm were recorded by using microplate reader (BioTeck Synergy 2). At the same time, the fluorescence imaging of HeLa cells incubated with **1** or **5** (**1**, 10 μg/mL; **2**, 500 μg/mL) was recorded by a Maestro II *in vivo* imaging system (Caliper Life Sciences, Hopkinton, MA). One part of the cells were collected, embedded and made into TEM specimens, and then observed *via* a TEM (FEI Tecnai12) at 120 kV.

Cytotoxicity of nanofiber. The Cell Counting Kit-8 (CCK-8) assay was employed to determine the viabilities of cancer cells to verify the cytotoxicity of **5**. Cell viabilities were normalized by control group without any treatment. HeLa or 4T1 cells were seeded at a density of 5000 cells per well in 96-well plates for 24 h, and then incubated with **1** at 10 μg/mL and **2** at 10~500 μg/mL for another 24 h. The standard CCK-8 assay was then carried out to evaluate the cell viability. Results were averaged from five independent replications.

NIR laser-induced Heat Conversion. The aqueous solutions of samples were stored in Eppendorf tubes, and irradiated upon 808 nm laser (1 W/cm^2, 3 min). The laser spot was adjusted to cover the whole surface of the samples. Real-time thermal imaging was recorded by a FLIR thermal camera. The temperature changes of samples were then analyzed by FLIR Examiner software.

***In vitro* NIR laser-induced PTT effect.** For *in vitro* PTT, HeLa cells were seeded at a density of 5000 cells per well in 96-well plates for 24 h, incubated with **1** or **5** (**1**, 10 μg/mL; **2**, 500 μg/mL) for 4 h, and irradiated by an 808 nm laser at different power densities (0.05, 0.1, 0.25, 0.5, and 1 W/cm^2) for 3 min. The cells were then incubated for another 24 h. The viabilities were evaluated by the standard CCK-8 assay. Dark control groups were kept identical to the experimental group except for illumination. Results were averaged from five independent replications.

Another parallel cell experiment included four groups: control, laser only, 5 only, and 5 + laser. HeLa cells were seeded at a density of 5000 cells per well in 96-well plates for 24 h, and incubated with **5** (**1**, 10 μg/mL; **2**, 500 μg/mL) for 4 h. Then the cells were illuminated by an 808 nm laser (1 W/cm^2, 5 min). Afterwards, the treated cells were co-stained with Calcein AM and propidium iodide (PI) for 30 min, washed with PBS, and imaged by an Olympus IX81 motorized inverted microscope.

Preparation of PEG based polymer gel disc with embedded alkaline phosphates (ALP). 0.5 mL of 7 wt% of PEGDA (Mw. 700) solution was mixed with DMPA (0.05 wt%) and 10 μL ALP (50 kU/mL), then placed in a plastic petri dish which has a well with a diameter of 1.5 cm. The mixture was exposed to a hand-held UV light (emission 365 nm) for 5 minutes. The PEG chains were cross linked *via* photo initiation and the polymer gel was formed instantly. The as-prepared PEG gel disc was thoroughly washed with DI water to get rid of un-reacted components and ALP on the surface before use.

PEG gel incubated with ICG or ICG plus precursor. The as-prepared PEG gel disc was placed in 5 mL ICG (10 μg/mL) solution or 5 mL solution containing ICG (10 μg/mL) and precursor (1 mg/mL) and incubated for 1 hour. The gel disc was next rinsed with DI water and cut. The micro-morphology on the cutting edge (the inner face) was inspected by SEM with Au

coating.

Animal models. All animal operations were performed according to institutional animal use and care regulations approved by the National Institutes of Health Clinical Center Animal Care and Use Committee (NIH CC/ACUC). Athymic female nude mice (six weeks old, 20-25 g) were obtained from Harlan (Indianapolis, IN). Tumor-bearing mice were established by subcutaneously injecting a suspension of 2×10^6 HeLa or 4T1 cells in PBS (60 μL) into the front flank of each nude mouse. The tumor-bearing mice were used for imaging and PTT treatment once the tumor volume reached around 60 mm^3.

***In vivo* fluorescence imaging.** During the image acquisition process, the mice were anesthetized with 1.0–2.0% isoflurane in oxygen delivered at a flow rate of 1.0 L min^{-1}. After completion of the image acquisition, spectral unmixing yielded the pseudocolored images of the pure spectrum of ICG. Image pre-processing and analysis were performed using Maestro version 2.2 software. Regions of interest (ROIs) were drawn over whole tumor for quantitative comparison, and the average signal for each area was measured. Results were presented as mean ± S.D.

For 4T1 tumor-bearing mice, both intravenous and intratumoral injection of **1** or **1** + **2** were investigated, respectively. For intravenous injection, the same protocol as that of HeLa tumor-bearing mice was used. For intratumoral injection, 100 μL of **1** (40 μg/mL), or 100 μL of **1** + **2** (**1**, 40 μg/mL; **2**, 2 mg/mL, n = 4), was injected. Images were acquired at 1, 1.5, 2, 3, 24 and 48 h postinjection.

For the inhibitor group, tumor-bearing mice were prepared by subcutaneously injecting a suspension of 2×10^6 HeLa cells in PBS (60 μL) into the both front flanks of each female nude mouse. When the tumor volume reached around 60 mm^3, the phosphatase inhibitor (50 μL, 10 μmol/L CinnGEL 2Me in 0.1% DMSO) was intratumorally injected into left side tumors for 3

times (once a day) before treatment. Then the mice received intravenous injection with **1** + **2** (**1**, 10 mg/kg; **2**, 100 mg/kg, n = 4). Images were acquired at 0.5, 1, 4 and 24 h postinjection.

***Ex vivo* histological staining.** Tumors and major organ tissues were collected from HeLa-tumor bearing mice in different groups. They were fixed in a 4% formaldehyde solution at room temperature. Haematoxylin and eosin (H&E) staining was done by BBC Biochemical, Mount Vernon, WA. The slides were observed using a BX41 bright field microscopy (Olympus).

Statistical Analysis. Results were presented as mean and SD. Two-tailed paired and unpaired Student's *t* tests were used to determine differences within groups and between groups, respectively. *P* value < 0.05 was considered statistically significant.

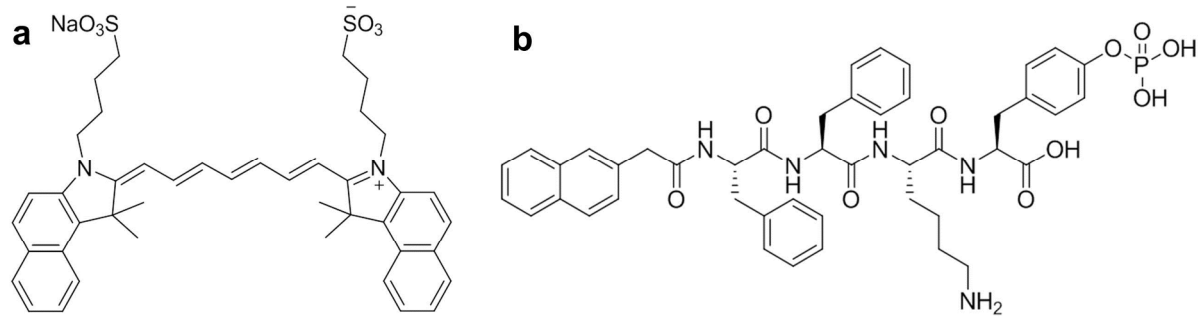

Scheme S1 Molecular structures of (a) ICG (**1**) and (b) NapFFKYp (**2**).

Scheme 1 shows the principle for enzyme-triggered supramolecular co-assembly of ICG **1** and NapFFKYp peptide precursor **2**. The precursor consists of a naphthyl group, two phenylalanines, one lysine, and one tyrosine phosphate residue. In the presence of the enzyme (such as alkaline phosphatase (ALP)), the tyrosine phosphate residue of **2** is cleaved by dephosphorylation reaction. Then precursor **2** turns into the gelator **3**, which, at above certain concentration, is able to self-assemble into nanofibers **4**. Our previous studies suggest that **2** also responds to the

cellular phosphatase over-expressed HeLa cells with high specific and efficiency, and form **4** at the cell level. When **1** is involved in the formation of **4**, **1** is spontaneously doped into **4** by J-aggregates forms with red-shifted and significantly enhanced absorbance, which is attributed to the strong intermolecular interaction between **1** and **3**. ICG-doped nanofibers **5** show enhanced NIR absorbance, partially self-quenched fluorescence emission, and improved photoacoustic and photothermal properties. With the aid of laser irradiation, **5** can efficiently convert optical energy into heat.

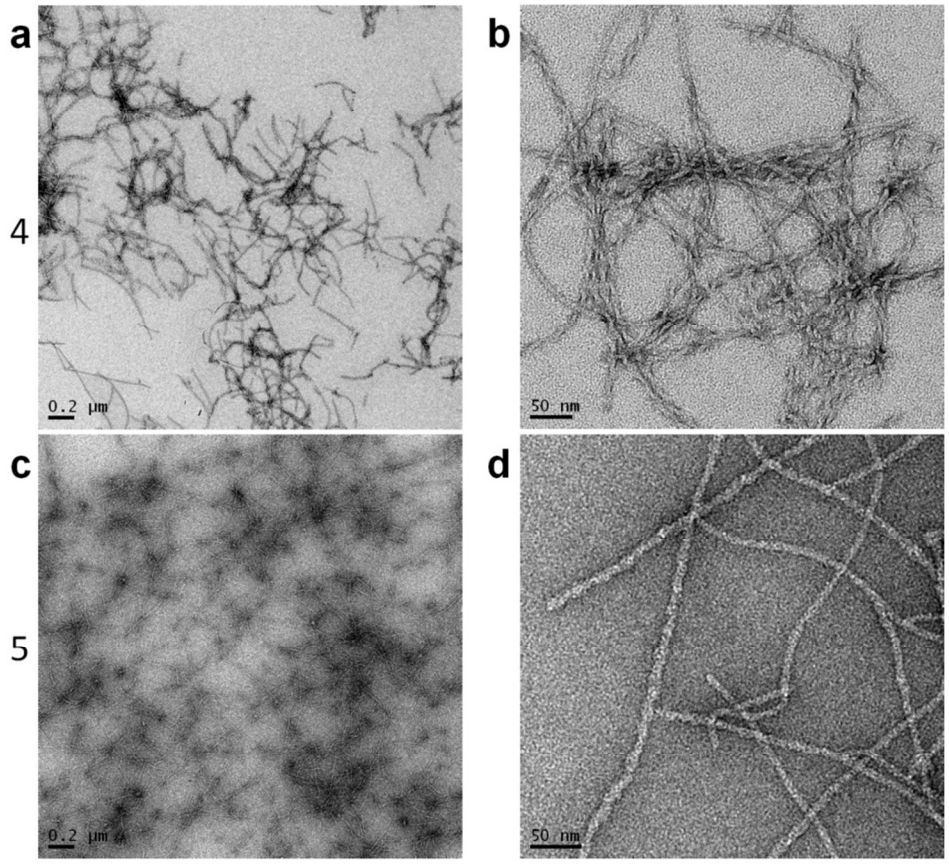

Figure S1. TEM images of negatively stained (a, b) nanofibers **4** and (c, d), ICG-doped nanofibers **5** (**1**, 10 μg/mL; **2**, 500 μg/mL).

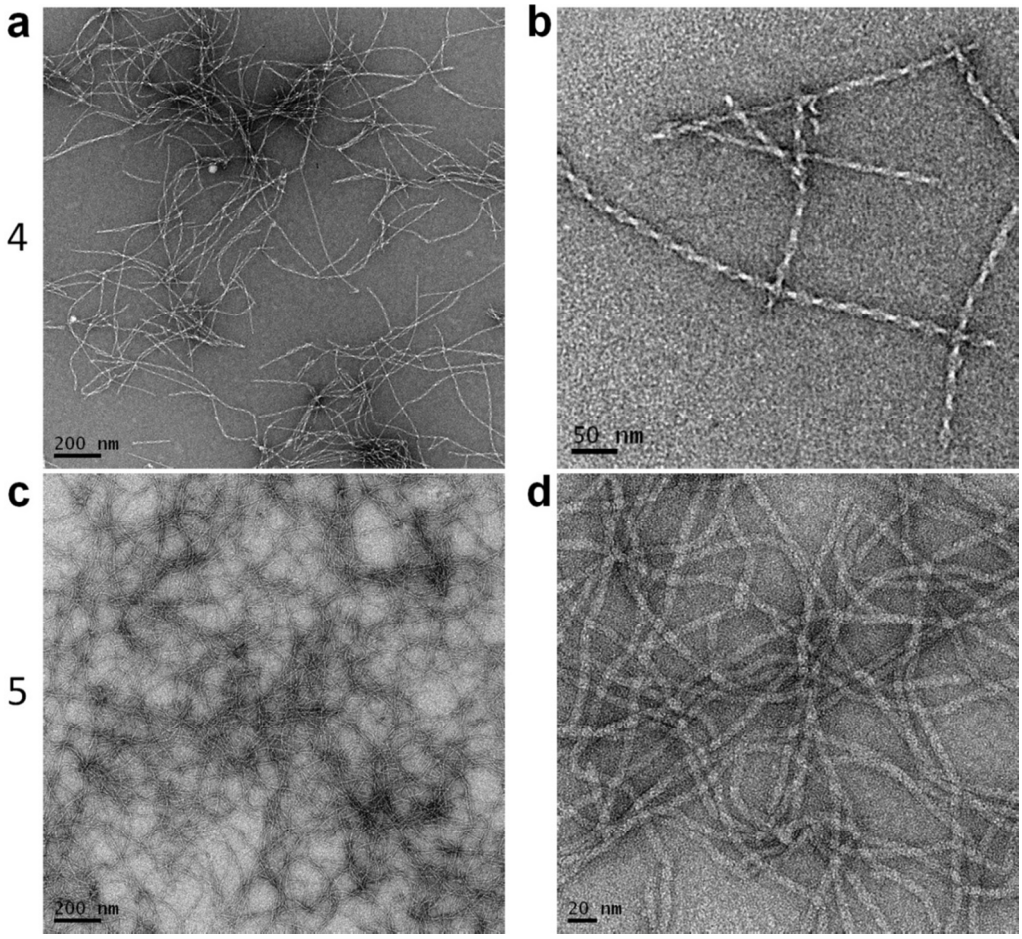

Figure S2. TEM images of negatively stained (a, b) nanofibers (**4**) and (c, d) ICG-doped nanofibers (**5**), (**1**, 10 μg/mL; **2**, 100 μg/mL).

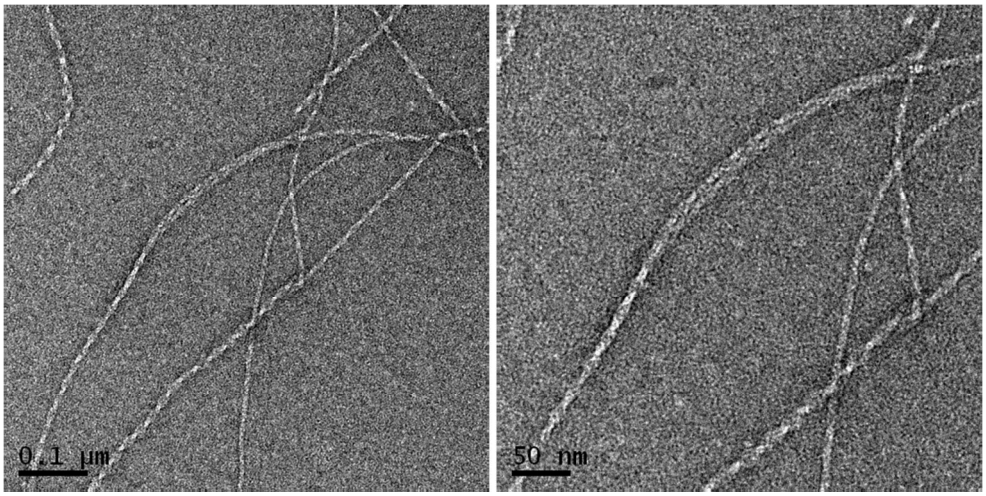

Figure S3. Representative TEM images of double helix nanofiber (**4**) (**2**, 100 μg/mL).

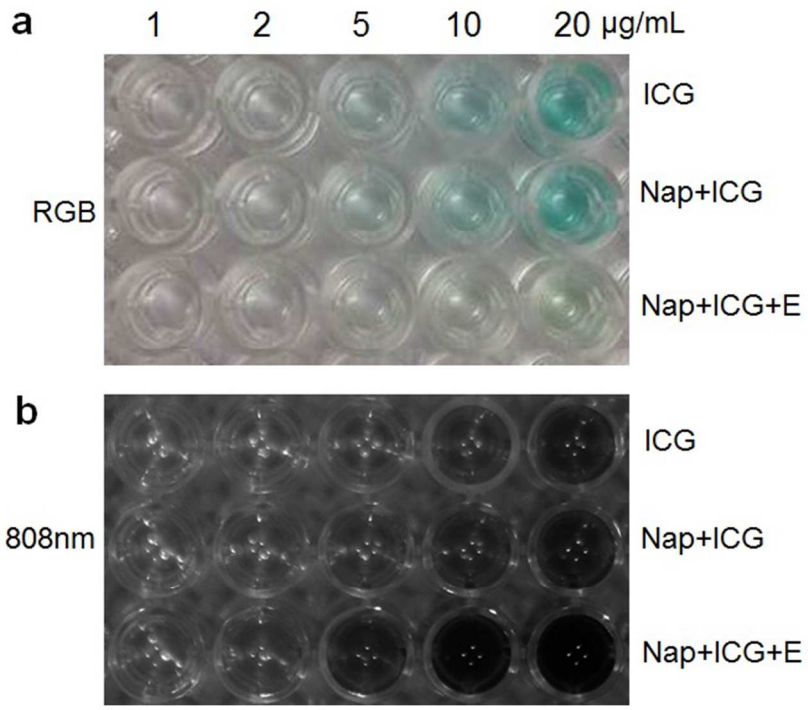

Figure S4. Photographs (a) RGB and (b) 808 nm of 1, 1+2, and 5 (**1** and **2** at the ratio of 1:100).

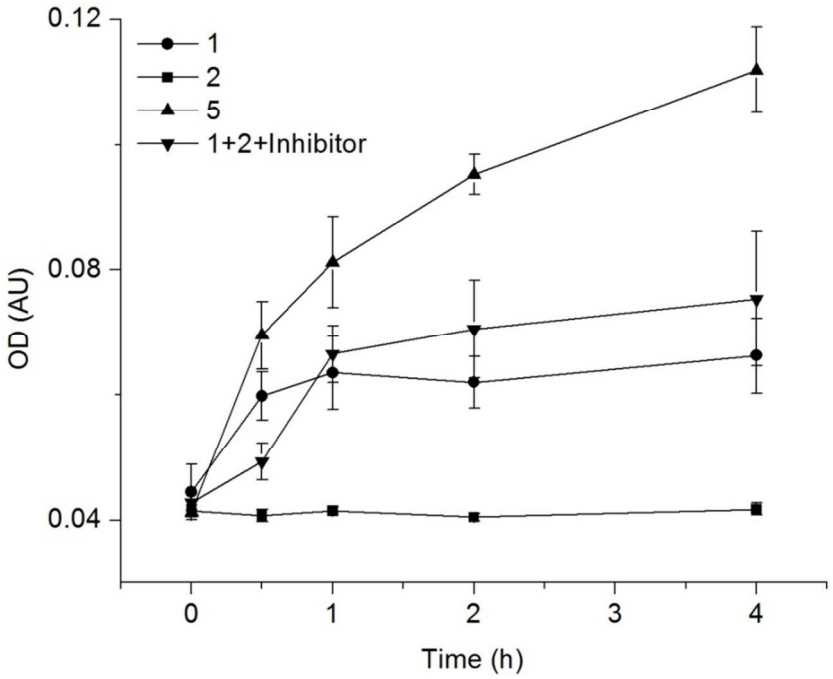

Figure S5. OD@780 nm changes of cellular phosphatase-triggered self-assembly on HeLa cells incubated with different samples (1, 10 μg/mL; 2, 500 μg/mL)

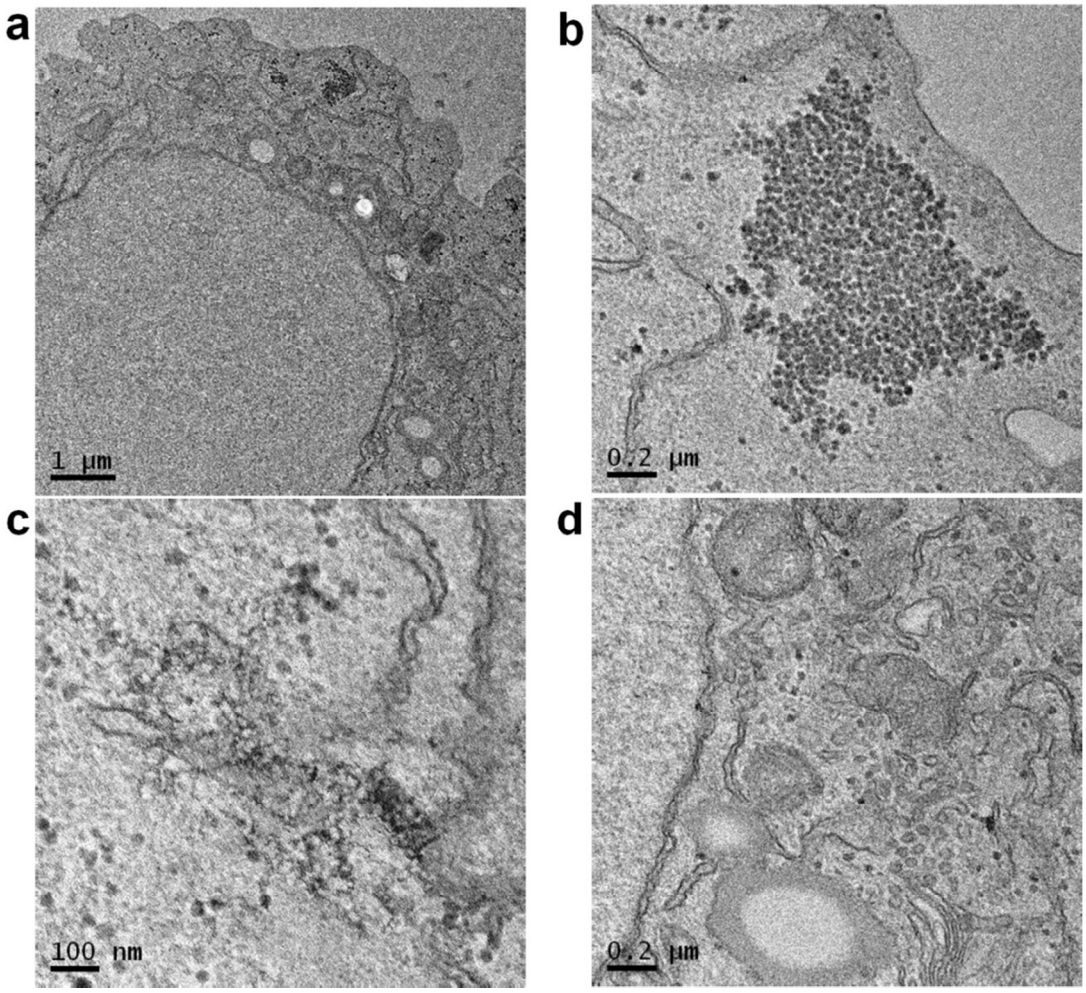

Figure S6. TEM images of the high-pressure frozen/freeze-substituted and plastic-sectioned HeLa cells that were incubated with 1 at 10 µg/mL and 2 at 500 µg/mL.

We also used TEM of high-pressure frozen/freeze-substituted HeLa cells to study the effects of the molecular assemblies on the cellular ultrastructure. We found the small vesicles with highly electron-dense substances and the large pools of the materials with low electron density. The small vesicles could be the lysosomes with the mixture of **1** and **2**. The large pools could be nanofibers **5**.

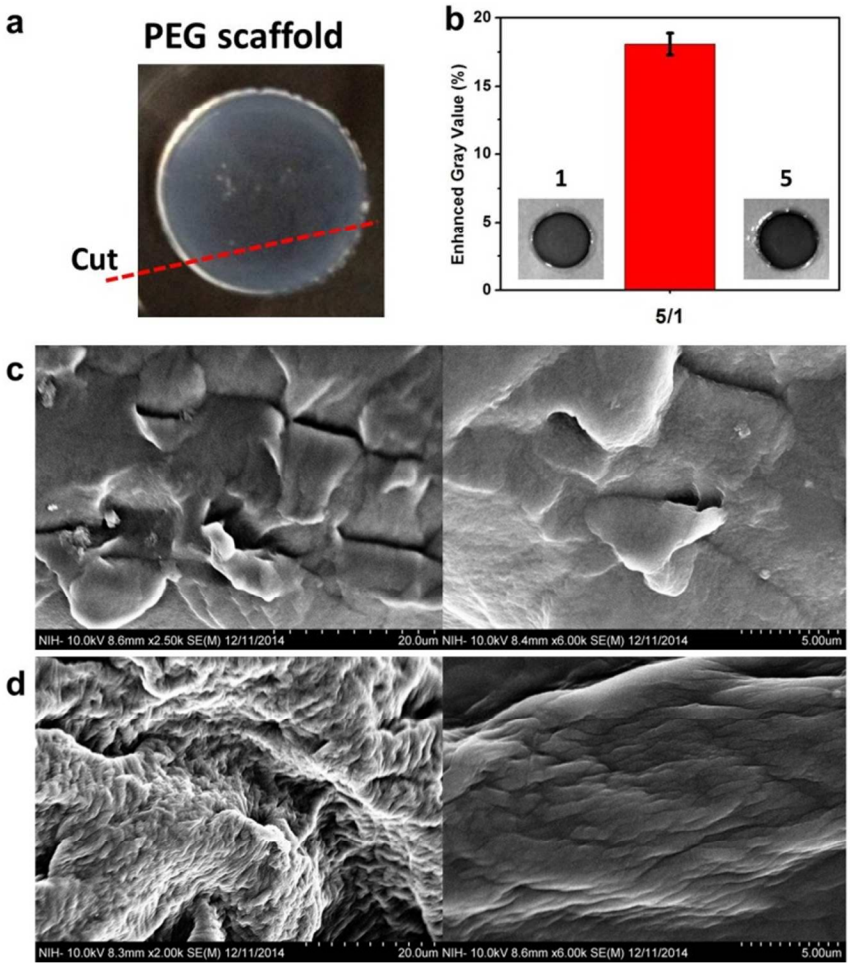

Figure S7. Artificial tissue of bioresorbable polymer scaffold with Enzyme. (a) The optical image illustrates the cutting edge of a PEG based polymer gel disc (diameter 1.5cm, thickness 0.3cm) embedding certain amount of alkaline phosphatase; (b) The gray value (OD at 808nm) ratio between a PEG gel immersed with ICG (**1**) or ICG (**1**) + precursor (**2**) which yields **5** after ALP catalysis; SEM images show the different surface roughness on the cutting edge of PEG gel with (c) **1** or (d) **5**.

Beyond the demonstration of the co-assembly of ICG with supramolecular nanofibers at the cell level, it is also essential to verify this process at tissue level which involves a much more complicated environment. As a starting point, we prepared a PEG based polymeric gel

containing alkaline phosphatase (ALP) which was trapped within gel matrix. PEG is the most widely used chemical serving as crowding agent and the PEG gel is likely to represent the crowded environment of a typical tissue. The presence of embedded ALP corresponds to the over-expression of phosphatase inside HeLa tumor. Sharing the feature of crowding effect and phosphatase activity, the as-prepared PEG gel matrix (Figure S7a) is designed to mimic a typical HeLa tumor at the minimum level. To verify the occurrence of co-assembly process in this PEG gel matrix, the PEG gel was then immersed in either solution of **1** or solution of **1** + **2** for one hour and rinsed before optical image were taken (Figure S7b). It is obvious that the right PEG gel (incubated with **1** + **2**) is darker than the left one. We used image-J to integrate the grey value of each piece of PEG gel and found that the grey value of the right one was 18% higher than the left one. As discussed earlier, the increase of the absorbance of ICG at 808 nm reflects the co-assembly of ICG into supramolecular nanofibers. Thus, the 18% increase of the grey value is attributed to the formation of **5** within this tissue mimic PEG gel matrix.

Further, we cut the treated PEG gel and used SEM to investigate the inner face and determine the micro morphology of **5** formed within PEG gel. As compared to Figure S7c, the appearance of the surface in Figure S7d is much rougher due to the presence of **5**. A closer look could tell the fibrillar morphology although the apparent fiber width is around 100 nm (nanofibers may aggregate during drying in sample preparation). Thus, we confirmed the co-assembly process of **1** and **2** to form **5** in a tissue mimic environment.

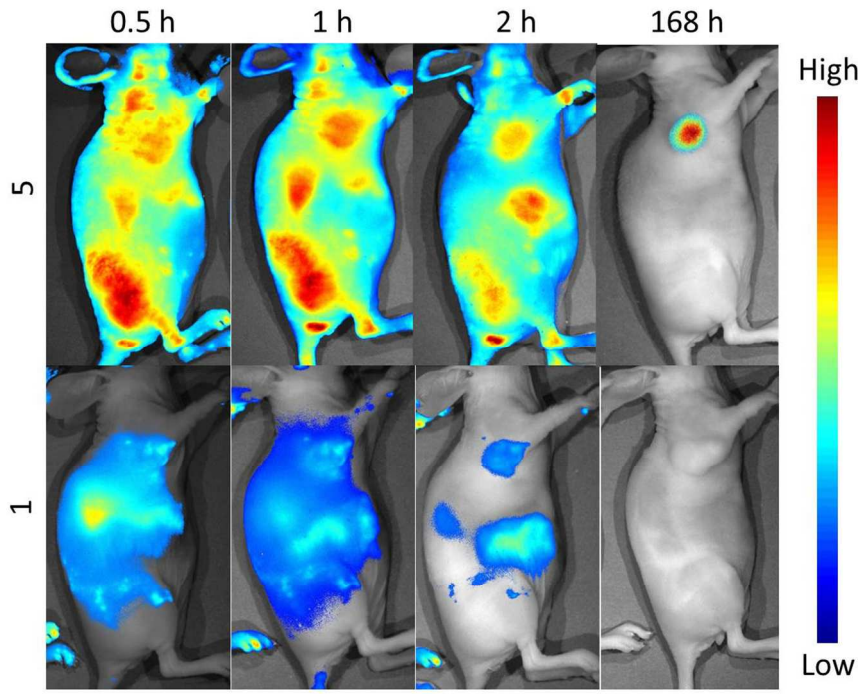

Figure S8 Representative NIR fluorescence images of 5 and 1 on Hela tumor-bearing mice after intravenous administration (1, 10 mg/kg, and 2, 100 mg/kg). Images were acquired at 0.5, 1, 2, and 168 h postinjection (p.i.).

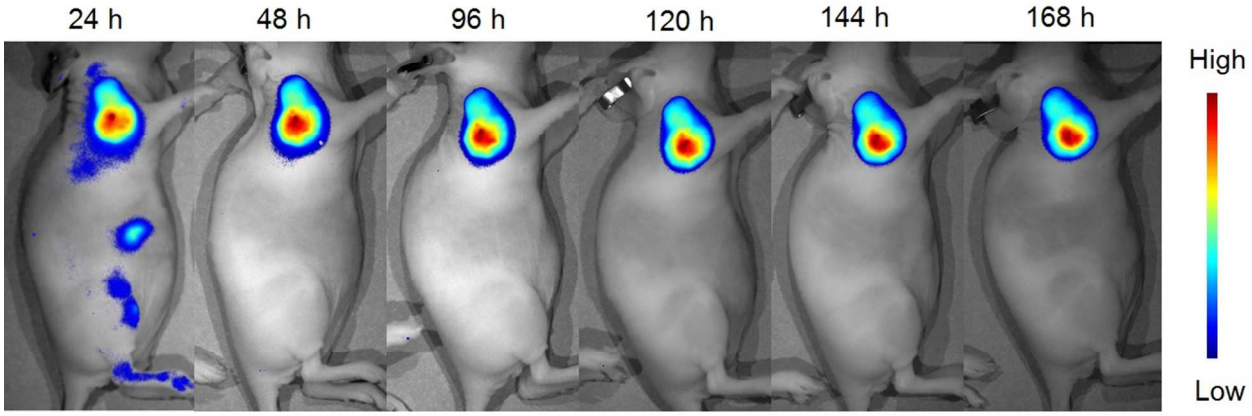

Figure S9 NIR fluorescence images of **5** on 4T1 tumor-bearing mice after intravenous administration (100 μL of **1**, 40 μg/mL, and **2**, 2 mg/mL). Images were acquired at 24, 48, 96, 120, 144 and 168 h postinjection (p.i.).

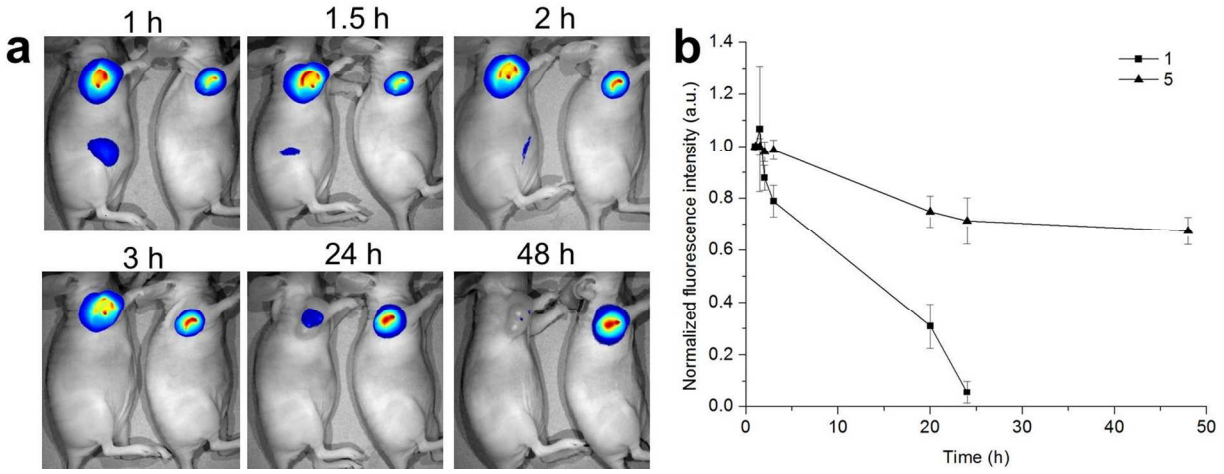

Figure S10 (a) NIR fluorescence images of **1** (Left) and **5** (Right) on 4T1 tumor-bearing mice after intratumoral administration (100 μL of **1**, 40 μg/mL, and **2**, 2 mg/mL). Images were acquired at 1, 1.5, 2, 3, 24 and 48 h postinjection (p.i.). (b) The normalized fluorescence intensity of tumor area as a function of time.

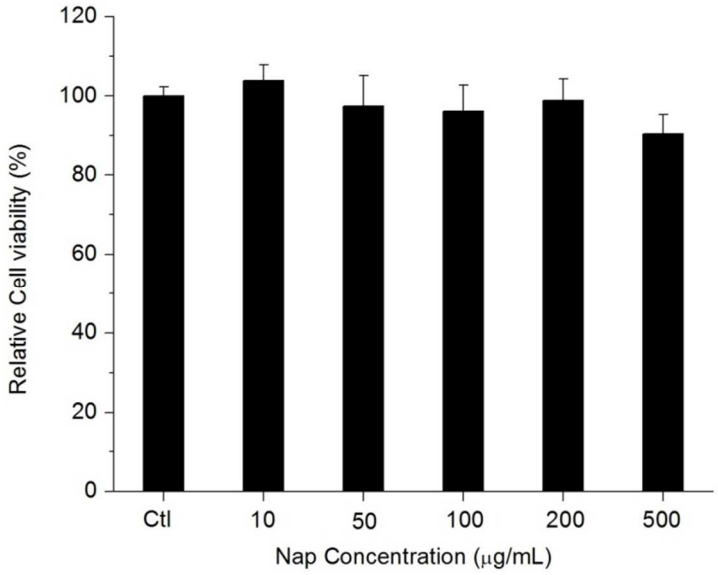

Figure S11 Relative viability of the HeLa cells after incubation with **5** for 24 h.

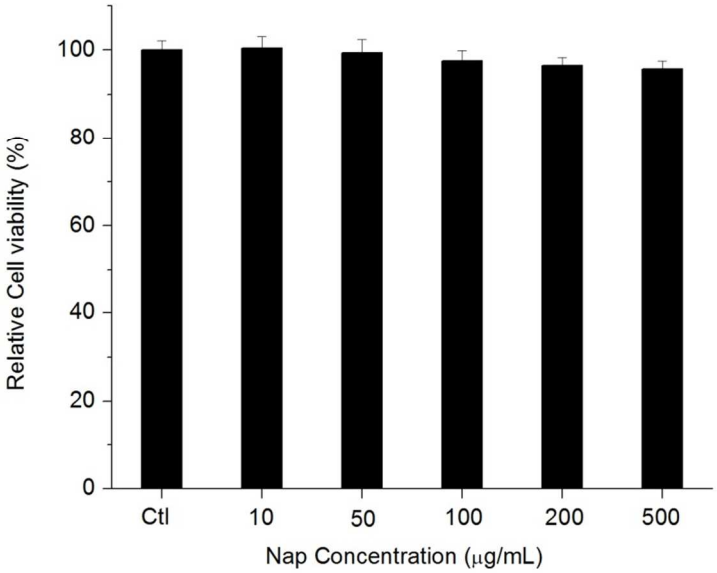

Figure S12 Relative viability of the 4T1 cells after incubation with **5** for 24 h.

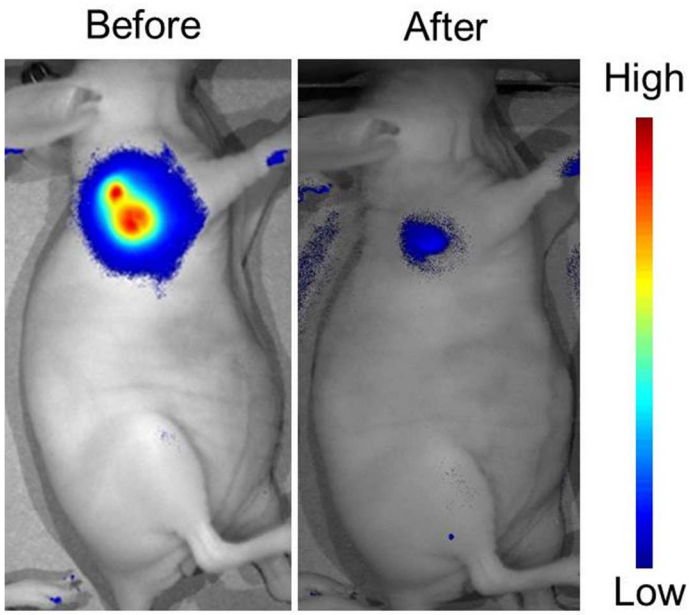

Figure S13 *In vivo* NIR fluorescence images of HeLa tumor-bearing mice before and after PTT treatment.

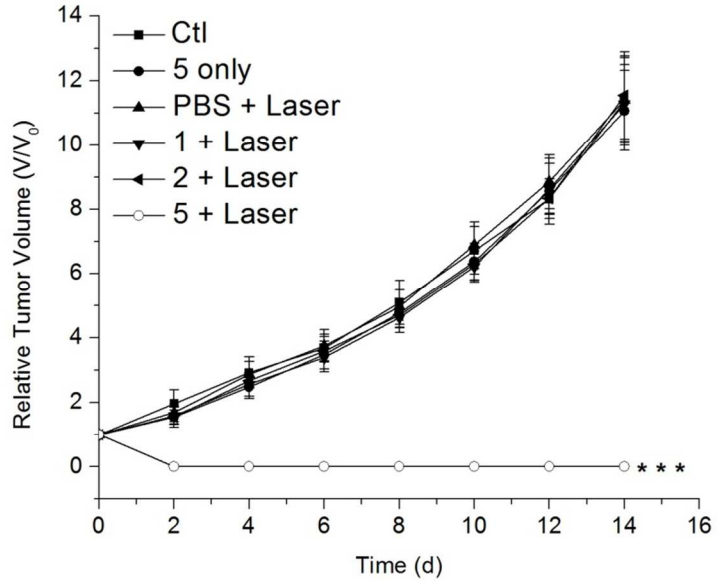

Figure S14 Tumor growth curves of different groups of 4T1 tumor-bearing mice after PTT treatment. Tumor volumes have been normalized to their initial sizes. Error bars represent the standard deviations of 5 mice per group. *** $P < 0.001$.

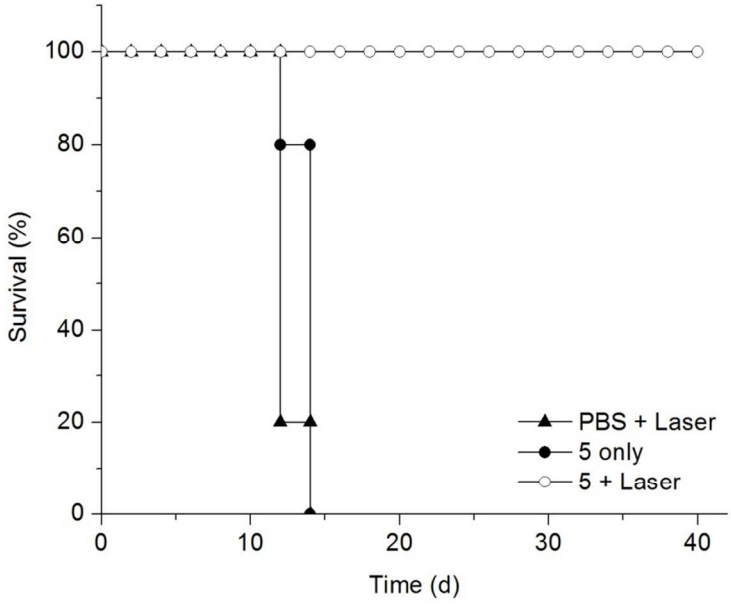

Figure S15 Survival curves of the 4T1 tumor-bearing mice after various treatments.

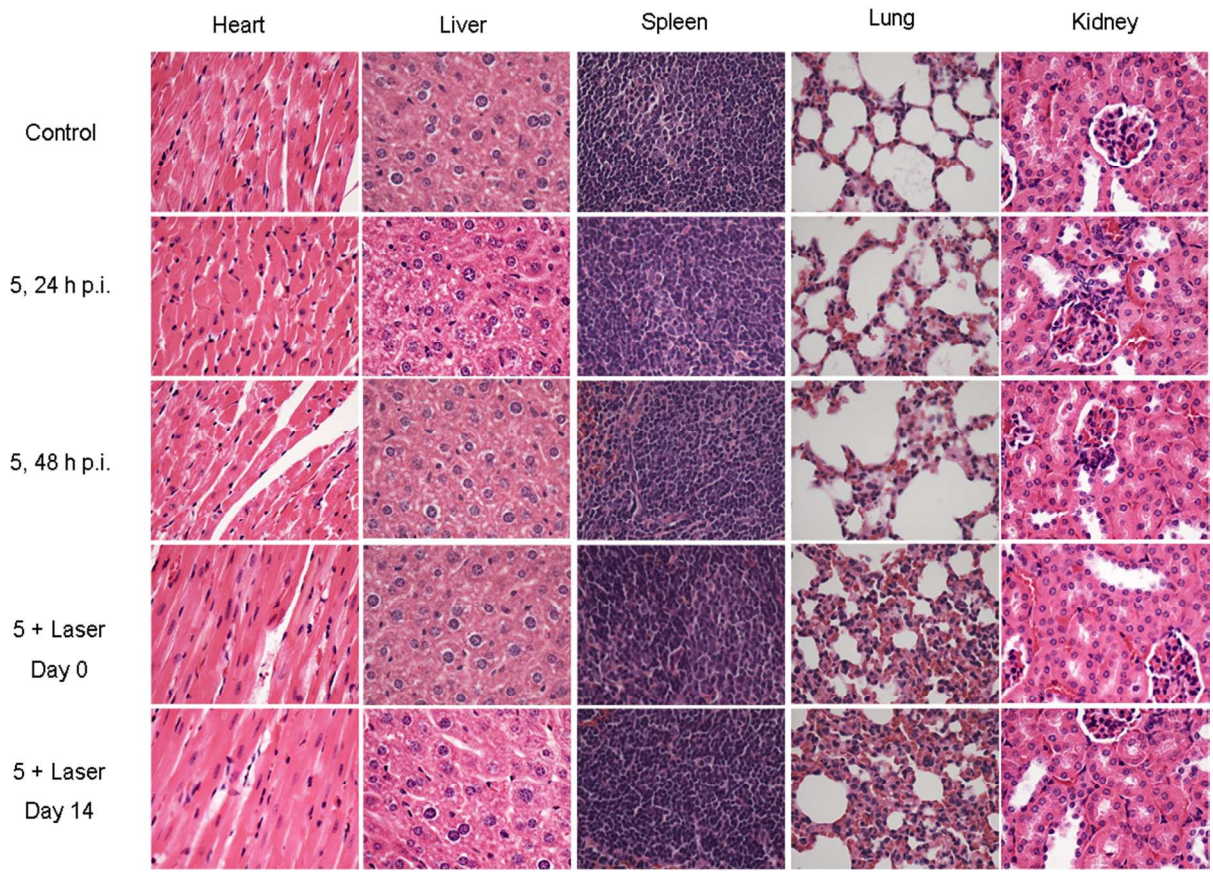

Figure S16 H&E stained images of major organs collected from different groups of HeLa tumor-bearing mice.